

The $\bar{q}q$ Bound States and Instanton Molecules at $T \gtrsim T_C$

Gerald E. Brown,^a Chang-Hwan Lee,^b Mannque Rho,^{c,d,e}
Edward Shuryak^a

^a*Department of Physics and Astronomy,
State University of New York, Stony Brook, NY 11794, USA
(E-mail: Ellen.Popenoe@sunysb.edu, shuryak@tonic.physics.sunysb.edu)*

^b*Department of Physics and
Nuclear Physics & Radiation Technology Institute (NuRI),
Pusan National University, Pusan 609-735, Korea
(E-mail: clee@pusan.ac.kr)*

^c*Service de Physique Théorique, CEA/DSM/SPhT. Unité de recherche associée au
CNRS, CEA/Saclay, 91191 Gif-sur-Yvette cédex, France
(E-mail: rho@sph.saclay.cea.fr)*

^d*School of Physics, Korea Institute for Advanced Study, Seoul 130-722, Korea*

^e*Department of Physics, Hanyang University, Seoul 133-791, Korea*

Abstract

The main objective of this work is to explore the evolution in the structure of the quark-anti-quark bound states in going down in the chirally restored phase from the so-called “zero binding points” T_{zb} to the full (unquenched) QCD critical temperature T_c at which the Nambu-Goldstone and Wigner-Weyl modes meet. In doing this, we adopt the idea recently introduced by Shuryak and Zahed for charmed $\bar{c}c$, light-quark $\bar{q}q$ mesons π, σ, ρ, A_1 and gluons that at T_{zb} , the quark-anti-quark scattering length goes through ∞ at which conformal invariance is restored, thereby transforming the matter into a near perfect fluid behaving hydrodynamically, as found at RHIC. We show that the binding of these states is accomplished by the combination of (i) the color Coulomb interaction, (ii) the relativistic effects, and (iii) the interaction induced by the instanton-anti-instanton molecules. The spin-spin forces turned out to be small. While near T_{zb} all mesons are large-size nonrelativistic objects bound by Coulomb attraction, near T_c they get much more tightly bound, with many-body collective interactions becoming important and making the σ and π masses approach zero (in the chiral limit). The wave function at the origin grows strongly with binding, and the near-local four-Fermi interactions induced by the instanton molecules play an increasingly more important role as the temperature moves downward toward T_c .

1 Introduction

1.1 $\bar{q}q$ bound states above T_c

The concept that hadronic states may survive in the high temperature phase of QCD, the quark-gluon plasma, has been known for some time. In particular, it was explored by Brown et al.[1,2]. The properties of (degenerate) π and σ resonances above T_c in the context of the NJL model was discussed earlier by Hatsuda and Kunihiro[3], and in the instanton liquid model by Schäfer and Shuryak [4]. Recently, lattice calculations [5,6] have shown that, contrary to the original suggestion by Matsui and Satz [7], the lowest charmonium states $J/\psi, \eta_c$ remain bound well above T_c . The estimates of the zero binding temperature for charmonium $T_{J/\psi}$ is now limited to the interval $2T_c > T_{J/\psi} > 1.6T_c$, where $T_c \approx 270\text{ MeV}$ is that for quenched QCD. Similar results for light quark mesons exist but are less quantitative at the moment. However since the “quasiparticle” masses close to T_c are large, they must be similar to those for charmonium states.

In the chiral limit ¹ all states above the chiral restoration go into chiral multiplets. For quark quasiparticles this is also true, but although the chirality is conserved during their propagation, they are not massless and move slowly near T_c where their “chiral mass” $m = E(p \rightarrow 0)$ is large ($\sim 1\text{ GeV}$).

RHIC experiments have found that hot/dense matter at temperatures above the critical value $T_c(\text{unquenched}) \approx 170\text{ MeV}$ is *not* a weakly interacting gas of quasiparticles, as was widely expected. Instead, RHIC data have demonstrated the existence of very robust collective flow phenomena, well described by ideal hydrodynamics. Most decisive in reaching this conclusion was the early measurement of the elliptic flow which showed that equilibration in the new state of matter above T_c set in in a time $< 1\text{ fm/c}$ [8]. Furthermore, the first viscosity estimates [9] show surprisingly low values, suggesting that this matter is the most perfect liquid known. Indeed, the ratio of shear viscosity coefficient to the entropy is only $\eta/s \sim 0.1$, two orders of magnitude less than for water. Furthermore, it is comparable to predictions in the infinite coupling limit (for $N=4$ SUSY YM theory) $\eta/s = 1/4\pi$ [10], perhaps the lowest value possible.

Shuryak and Zahed[11] (hereafter referred to as SZ whenever unambiguous) have recently connected these two issues together. They have suggested that large rescattering cross sections apparently present in hot matter at RHIC are

¹ In most of what follows, we will be ignoring the effect of light-quark masses, unless mentioned otherwise. The “quasiparticle mass” that we shall refer to in what follows is a chirally invariant object called “chiral mass.”

generated by resonances near the zero-binding lines. Indeed, at the point of zero binding the scattering length a of the two constituents goes to ∞ and this provides low viscosity. This phenomenon is analogous to the elliptic flow observed in the expansion of trapped ^6Li atoms rendered possible by tuning the scattering length to very large values via a Feshbach resonance [12].

Near the zero-binding points, to be denoted by T_{zb} , introduced by SZ the binding is small and thus the description of the system can be simple and nonrelativistic. The binding comes about chiefly from the attractive Coulomb color electric field, as evidenced in lattice gauge calculation of Karsch and collaborators[5,13], and Asakawa and Hatsuda[6], as we shall detail. The instanton molecule interactions, which we describe below, are less important at these high temperatures ($T \sim 400$ MeV). All this changes as one attempts (as we show below) to discuss the more deeply bound states just above T_c (unquenched).

In another work [14], Shuryak and Zahed have also found sets of highly relativistic bound light states in the strongly coupled $N=4$ supersymmetric Yang-Mills theory at finite temperature (already mentioned above in respect to viscosity). They suggested that the very strong Coulomb attraction can be balanced by high angular momentum, producing light states with masses $m \sim T$. Furthermore, the density of such states remains constant at arbitrarily large coupling. They argued that in this theory a transition from weak to strong coupling basically implies a smooth transition from a gas of quasiparticles to a gas of “dimers” ², without a phase transition. This is an important part of the overall emerging picture, relating strong coupling, viscosity and light bound states.

In this work we wish to construct the link between the chirally broken state of hadronic matter below T_c (unquenched) and the chirally restored mesonic, glueball state above T_c . Our objective is to understand and to work out in detail what exactly happens with hadronic states at temperatures between T_c and T_{zb} . One important new point is that these chirally restored hadrons are so small that the color charges are locked into the hadrons at such short distances (< 0.5 fm) that the Debye screening is unimportant. This is strictly true at $T \gtrsim T_c$, where there is very little free charge. In this temperature range the nonrelativistic treatment of SZ should be changed to a relativistic one.

The relativistic current-current interaction, ultimately related with the classical Ampere law, is about as important as the Coulomb one, effectively doubling the attraction (see section 2.1). We also found that the spin-spin forces discussed in 2.2 are truly negligible. In effect, with the help of the instanton

² In the large number of color limit considered, those are dominated by bound colored states, not colorless mesons that are important in the regime we are considering.

molecule interaction, one can get the bound quark-anti-quark states down in energy, reaching the massless σ and π at T_c , so that a smooth transition can be made with the chiral breaking at $T < T_c$.

The nonperturbative interaction from the instanton molecules becomes very important³. Let us remind the reader of the history of the issue. The nonperturbative gluon condensate, contributing to the dilatational charge or trace of the stress tensor $T_{\mu\mu} = \epsilon - 3p$, is not melted at T_c (unquenched). In fact more than half of the vacuum gluon condensate value remains at T right above T_c . the hard glue or epoxy which explicitly breaks scale invariance but is unconnected with hadronic masses. The rate at which the epoxy is melted can be measured by lattice gauge simulations, and this tells us the rate at which the instanton molecules are broken up with increasing temperature. We will discuss this further in section 1.3.

As argued by Ilgenfritz and Shuryak [16] (for further references see the review [15]), this phenomenon can be explained by breaking of the instanton ensemble into instanton molecules with zero topological charge. Such molecules generate a new form of effective multi-fermion effective interactions similar to the original NJL model, see details in section 2.3. Brown et al.[17] (denoted as BGLR below) obtained the interaction induced by the instanton molecules above T_c by continuing upwards the Nambu-Jona-Lasinio description from below T_c .

Our present discussion of mesonic bound states should not be confused with quasi-hadronic states found in early lattice calculations[18] for quarks and anti-quarks propagating in the space-like direction. Their spectrum, known as “screening masses” is generated mostly by “dynamical confinement” of the spatial Wilson loop which is a nonperturbative phenomenon seen via the lattice calculations. Similar effects will be given here by the instanton molecule interaction. We will briefly discuss it in section 1.4.

1.2 Quasiparticles and their masses at $T > T_c$

It is well known that the expectation value of the Polyakov line $|\langle L \rangle|$ goes to zero at T_c , indicating an infinite quark mass below T_c ; i.e., confinement. In the deconfined phase we discuss this mass is finite, and as T grows it is expected to decrease to some minimal value, before growing perturbatively as $M \sim gT$ at large T .

Chirality of the quarks is a good quantum number above T_c . Now the chirally restored wave functions have good helicity, $+$ or $-$. Also it can be seen from

³ Although we do not discuss $T < T_c$ in this work, we still mention that in this region the instanton-induced effects seem to become dominant, see [15] for review.

eq. (9) that each wave function has good chirality, $\vec{\sigma} \cdot \vec{p} \psi = \pm p \psi$. The helicities and chiralities use up the 4 components in the Dirac wave function. The fermion modes with equal (opposite) helicities and chiralities are called “quark quasiparticles” (“plasmino” modes).

There are detailed results on their dispersion relations from pQCD. Specifically for quark quasiparticles, Weldon[19] obtained the dispersion relation

$$p_0 - |\vec{p}| = \frac{M_{th}^2}{|\vec{p}|} \left(1 + \left(1 - \frac{p_0}{|\vec{p}|} \right) \frac{1}{2} \ln \left(\frac{p_0 + |\vec{p}|}{p_0 - |\vec{p}|} \right) \right) \quad (1)$$

which can be reasonably well approximated (to within 10%) by $p_0^2 \approx M_{th}^2 + \vec{p}^2$ where $M_q^2 \equiv g^2 T^2 / 6$. The perturbative gluon mass is $M_g^2 \equiv g^2 T^2 (N_c/2 + N_f/6)/2$ [20].

If the exact dispersion relations for quasiparticles are known, the 2-body interaction can be introduced by standard substitution of frequency and momenta by the covariant derivatives with the potentials.

Unfortunately, the actual lattice data about the masses are very fragmented, and are (to our knowledge) only available from quenched calculations. The Polyakov loop expectation value $|\langle L \rangle|(T)$ is plotted in Asakawa et al.: at each N_τ it starts to deviate from zero at $T_c \sim 270$ MeV, the critical temperature for quenched calculations. However, one has to renormalize the mass, removing the linear divergent part of the point charge mass $\sim 1/a$ before extracting any numbers, which needs more data.

There are some results on quasiparticle dispersion relations from Petreczky et al. [13], who find in (quenched) calculation that they are all consistent with the usual dispersion relation $\omega^2 = k^2 + m^2$ with the masses $m_q/T = 3.9 \pm 0.2$, $m_g/T = 3.4 \pm 0.3$ or $m_q \sim 1.6$ GeV, $m_g \sim 1.4$ GeV for $T = 1.5T_c = 405$ MeV where we take $T_c = 270$ MeV. These quarks (and gluons) are about as massive as charmed quarks. Although obviously these masses will be reduced in unquenched calculations, probably roughly by the ratio of critical temperatures or so, it seems inevitable that at $T \gtrsim T_c$ the quarks are so massive ⁴ that their Boltzmann factors are small, inadequate to furnish substantial presence of free quarks and gluons. The light bound state would then be primary sources of the pressure, as at low T .

Petreczky et al.[13] omitted the first three values (at lowest temperatures) from their fit of $\omega_q(p)$. Their curve of $\omega_q^2(p)/T^2$ intercepts the ordinate at a

⁴ We will argue for a somewhat lower values below, which would perhaps arise from the unquenched calculations. Let us also remember that those are the “chiral masses” which do not break chiral symmetry.

value of ~ 9 , which would give $\omega_q(p) \sim 3T$, or ~ 1.2 GeV. Furthermore, their m_q are calculated with bare quark masses which increases m_q , whereas our calculations are in the chiral limit. At least for the moment, our use of $m_q = 1$ GeV seems not unreasonable.

In spite of such large uncertainties in the mass, we will be able to carry out the calculations of meson binding, expressing it in units of $m_q(T)$, so that its precise value won't matter. In particular, we will show that at $T \rightarrow T_c$ (*unquenched*) the binding of the pion and sigma mesons will go to $-2m_q(T)$, making them massless. The spin-spin and instanton molecule interaction will at this point be less attractive for vector and axial mesons, which will thus have a finite limit⁵ of $M_{V,A}/m_q$ at $T \rightarrow T_c$.

1.3 The “hard glue” and instanton molecules at $T > T_c$

As we already mentioned in the introduction, the trace of the stress tensor $T_{\mu\mu} = \epsilon - 3p$, is not “melted away” at $T > T_c$, but is instead only a factor 2 smaller than at $T = 0$. Nice details on this observable have been recently provided by David Miller[23], who used a set of the Bielefeld group lattice data and showed that the hard glue is only melted by $T \lesssim 400$ MeV.

The natural explanation of the existence of such “hard glue” or “epoxy” component, which survives chiral restoration and deconfinement, was given by the theory of instantons. It has been argued [16] that chiral restoration is not related to the instanton suppression at $T > T_c$, as was previously thought, but to their rearrangement, from the quasi-random ensemble to that made of correlated instanton-anti-instanton pairs (or other clusters with net zero topological charge). Some details of the quantum/statistical mechanics of a $\bar{I}I$ molecules can be found in [24], the finite T simulations of instanton ensemble has been shown in [25], for other references see [15].

For a single molecule the contribution to the partition function can be written as

$$Z = \int d\Omega d\bar{\Omega} |T_{\bar{I}I}|^{2N_f} \exp(-S_g) \quad (2)$$

where $\Omega, \bar{\Omega}$ are 12-dimensional collective variables for I, \bar{I} , namely size, 4 po-

⁵ Note however that the Harada-Yamawaki vector manifestation (VM) [21] of chiral symmetry predicts that the vector mesons also reach zero mass at T_c from below in accordance with the BR scaling. In a forthcoming publication [22], an argument will be developed to the effect that the vector mesons also go massless as $T \rightarrow T_c$ from above.

sitions and 7 $SU(3)_c$ angles⁶. Here T_{II} is the matrix element of the Dirac operator between 2 zero modes, that of the instanton and anti-instanton.

Instead of evaluating the coupling constant from first principles, one can do in phenomenologically, in a NJL-like framework. Brown et al [17] (BGLR) showed that the scaled attraction which breaks chiral symmetry below T_c gives way to one only slightly ($\sim 6\%$) lower in which chiral symmetry is restored at T_c (unquenched). Whereas the Nambu Jona-Lasinio (NJL) below T_c was connected to the “soft glue” part of (which may be associated with the spontaneously generated part of⁷) the scale anomaly which gets restored with chiral symmetry, at least half, if not more, of the glue – which we called “epoxy” – remained at T_c and for some distance above, being melted only gradually with increasing T . The “hardness” of this glue explains why $T_c(\text{quenched})$ is so much higher (by nearly 50 %) than $T_c(\text{unquenched})$.

1.4 The “screening” masses and states

The issue was raised first by DeTar et al [18] and explained by Koch et al.[30]. The “screening” states are formed due to a specific nonperturbative phenomena in the magnetic sector of high- T QCD related with “dynamical confinement of spatial Wilson loops”. These phenomena exist at all $T > T_c$ and are best explained [30] in a “funny space” in which the coordinates t and z had been interchanged. In this way the new “temperature” in the old z direction was zero, whereas the new z is compactified to $(\pi T)^{-1}$, essentially a

⁶ One of the angles conjugated to the Gell-Mann matrix λ_8 , does not rotate the instanton solution since it has only 2 colors.

⁷ An elaboration is perhaps in order on the nature of symmetry breaking involved here with the conformal invariance. As mentioned above and elsewhere [17,26], the trace anomaly of QCD associated with the scale symmetry breaking has, roughly speaking, two components: One “soft” component which is locked to chiral symmetry and the other “hard” or “epoxy” component which is not directly tied to chiral symmetry. In fact in [26], it was explicitly shown how in dense medium the soft component “locks onto” the property of chiral symmetry, with the melting of the soft component corresponding to the melting of the quark condensate. This is the notion used in the early discussion of BR scaling [27]. The simplest way to understand this phenomenon in the case at hand is to consider the soft component as resulting from an “induced (or spontaneous) symmetry breaking” and the hard component as an explicit symmetry breaking of conformal symmetry. As is known since a long time [28], conformal symmetry can be spontaneously broken *only if* it is also explicitly broken. Thus we can identify the soft component of the glue that melts across the phase transition as arising from spontaneous breaking *in the presence of* an explicit breaking which remains intact across the phase boundary. This is analogous to “induced symmetry breaking (ISB)” of Lorentz symmetry in the presence of chemical potential discussed in [29].

dimensional reduction.

In the Koch et al. work[30], in the old time (new z direction), the Coulomb potential came from a periodic array of charges, because of the periodicity in this direction, which in the large- T limit became that from a wire

$$\Phi(r_\perp) = -\frac{g}{2\pi\beta} \ln(r_\perp/2\beta) \quad (3)$$

where $\beta = T^{-1}$. Such a potential had earlier been obtained in QCD by Hansson & Zahed [31].

A linearly rising potential from the space-like string tension was added, because it was felt that confinement on top of the logarithmic attraction was needed to hold the quark and anti-quark together. The $-g^2(\vec{\alpha}_1 \cdot \vec{\alpha}_2/r)$ interactions were, however, in the two-dimensional x, y directions in the disc through current loops, and give about one eighth of the attraction we shall find. Another eighth, as we outline below, comes from the usual Coulomb attraction which goes as $-g^2/r$ at larger distances, and which is sufficient to bind the quark and anti-quark. The largest part of the binding around T_c comes from the instanton molecule interaction.

Koch et al.[30] ignored the effective Coulomb interaction (in the 2d form of that from a charged wire) because of the dominance of the space-like string tension. Putting together the above forces produced the two-dimensional π and ρ wave functions in the x, y -plane. Since the x and y directions were unchanged, on this plane we should recover these same wave functions in a projected four-dimensional QCD calculation, but with increased binding because of the additional interactions included.

The important feature of DeTar's spatially propagated states was that quarks were still confined in colorless states above T_c (unquenched) [18]. However in our work we discuss real propagating states, and so in the deconfined phase, $T > T_c$, those can be colored. The non-singlet $\bar{q}q$ states are only the color octet ones, which is a channel with color repulsive force and is obviously unbound: but states made of qg and gg type have colored channels with an attraction and should exist. One more famous example of colored bound states is the qq Cooper pairs, leading to color superconductivity phases [32]. Although we could have discussed all of them in the same way as we did the $\bar{q}q$ ones, we defer this discussion to future works. The 32 lowest $\bar{q}q$ states we consider here are, however, colorless.⁸ Thus in the temperature region up to $\sim 2T_c$

⁸ In total, there are 32 degrees of freedom of the $\bar{q}q$ bound states which lie in mass well below the masses of quarks and gluons, and are therefore the relevant variables for the thermodynamics. This is somewhat fewer than the 37 equivalent boson degrees of freedom arising from perturbative quarks and gluons. This may be

(unquenched), essentially up to the temperatures reached by RHIC, we have a dynamical color confinement.

2 Binding of the $\bar{q}q$ states

2.1 The Coulomb interaction and the relativistic effects

At $T > T_c$ the charge is screened rather than confined [20], and so the potential has a general Debye form

$$V = \frac{\alpha_s(r, T)}{r} \exp\left(-\frac{r}{R_D(T)}\right) \quad (4)$$

(Note that we use a (somewhat nonstandard) definition in which α_s absorbs the 4/3 color factor.) The general tenet of QCD tells us that the strength of the color Coulomb should run. We know that perturbatively it should run as

$$\alpha_s \sim \frac{1}{\log(Q/\Lambda_{\text{QCD}})} \quad (5)$$

with $\Lambda_{\text{QCD}} \sim 0.25$ GeV. The issue is what happens when the coupling is no longer small. In vacuum we know that the electric field is ultimately confined to a string, producing a linear potential.

In the plasma phase this does not happen, and SZ assumed that the charge runs to larger values, which may explain the weak binding at rather high T we discussed in the introduction. Lattice results produce potentials which, when fitted in the form $V(r) = -A \exp(-mr) + B$ with constant A, B indeed indicate⁹ that $A(T)$ grows above T_c until its maximum at $T = 1.4 T_c$, before starting to decrease logarithmically at high T . The maximal value of the average¹⁰ coupling $\max(A) \approx 1/2$. This is the value which will keep charmonium bound, as found by Asakawa and Hatsuda, up to $1.6 T_c$ [6].¹¹

a partial explanation of the $\sim 20\%$ lower number of degrees of freedom than would result from quarks and gluons, found in lattice calculations.

⁹ We thank Stefano Fortunato for useful discussion of the issue and for the fits he provided to us.

¹⁰ The maximal value of the running coupling in SZ was taken to be 1, but its value at the most relevant distances is about 1/2 also.

¹¹ We thank L  ic Grandchamps for this calculation.

Running of the coupling is not very important for this work in which we are mostly interested in deeply bound states related with short enough distances. Therefore we will simply keep it as a non-running constant, selecting an appropriate average value.

It is well known in the point charge Coulomb problem (QED) that when $Z\alpha$ is increased and the total energy reaches zero there is a singularity, preventing solutions for larger $Z\alpha$. In the problem of the “sparking of the vacuum” in relativistic heavy ion collisions, the solution of the problem was found by approximating the nuclei by a uniformly charged sphere; for a review of the history see Rafelski et al. [33]. As a result of such regularization, the bound electron level continues past zero to $-m$, at which point e^+e^- production becomes possible around the critical value of $Z_{cr} = 169$. In short, the problem of the point Coulomb charge could be taken care of by choosing a distributed electric field which began from zero at the origin.

In QCD the charge at the origin is switched off by asymptotic freedom, the coupling which runs to zero value at the origin. A cloud of virtual fields making the charge is thus “empty inside”. We will model a resulting potential for the color Coulomb interaction by simply setting the electric field equal to zero at $r = 0$, letting it decrease (increase in attraction) going outward ¹². We can most simply do this by choosing a charge distribution which is constant out to R , the radius of the meson. If the original $2m_q$ mass were to be lowered to zero by the color Coulomb interaction and instanton molecule interaction, then the radius of the final molecule will be

$$R \simeq \frac{\hbar}{2m_q}, \quad (6)$$

although the rms radius will be substantially greater with the instanton molecule interactions playing the main role around T_c .

$$\begin{aligned} V &= -\alpha_s \frac{1}{2R} \left(3 - \frac{r^2}{R^2} \right), & r < R \\ &= -\alpha_s \frac{1}{r}, & r > R. \end{aligned} \quad (7)$$

This V has the correct general characteristics. As noted above, the electric field \vec{E} must be zero at $r = 0$. It is also easy to see that V must drop off as r^2/R^2 as

¹²Just at $r = 0$ the quark and anti-quark are on top of each other, so the electric field is clearly zero. (Although the quark and anti-quark are point particles, their wave functions will be distributed.) For two rigid spheres, V would take up the $1/r$ behavior only at $2R$, but there will be some flattening. It will become clear that our main conclusions are independent of these details.

the two spheres corresponding to the quark and anti-quark wave functions are pulled apart. Precisely where the potential begins the $1/r$ behavior may well depend upon polarization effects of the charge, the + and – charges attracting each other, but it will be somewhere between R and $2R$, since the undisturbed wave functions of quark and anti-quark cease to overlap here.

The $q\bar{q}$ system is similar to positronium in the equality of masses of the two constituents. Since the main term value is¹³ $m\alpha^2/4$, the 4, rather than 2 in hydrogen, coming from the reduced mass, one might think that the Coulomb, velocity-velocity and other interactions would have to be attractive and 8 times greater than this term value in order to bring the $2m_q$ in thermal masses to zero. However, this does not take into account the increase in reduced mass with α . Breit and Brown [34] found an $\alpha^2/4$ increase in the reduced mass with α , or 25% for $\alpha = 1$, to that order. It should be noted that in the Hund and Pilkuhn [35] prescription the reduced mass becomes $\mu = m_q^2/E$, which increases as E drops.

We first proceed to solve the Coulomb problem, noting that this gives us the solution to compare with the quenched lattice gauge simulations, which do not include quark loops.

Having laid out our procedure, we shall proceed with approximations. First of all, we ignore spin effects in getting a Klein-Gordon equation. The chirally restored one-body equation which has now left-right mixing is given by

$$(p_0 + \vec{\alpha} \cdot \vec{p})\psi = 0. \quad (8)$$

Expressing ψ in two-component wave functions Φ and Ψ , one has

$$\begin{aligned} p_0\Phi &= -\vec{\sigma} \cdot \vec{p}\Psi \\ p_0\Psi &= -\vec{\sigma} \cdot \vec{p}\Phi, \end{aligned} \quad (9)$$

giving the chirally restored wave function on Ψ

$$\left(p_0 - \vec{\sigma} \cdot \vec{p} \frac{1}{p_0} \vec{\sigma} \cdot \vec{p} \right) \Psi = 0. \quad (10)$$

Here

$$p_0 = E_V = E + \alpha_s/r. \quad (11)$$

¹³ To make comparison with QCD we should use $Z^2\alpha$ rather than α and remember the Casimir factor $4/3$.

Neglecting spin effects, $\vec{\sigma} \cdot \vec{p}$ commutes with p_0 , giving the Klein-Gordon equation $p_0^2 - \vec{p}^2 = 0$. We now introduce the effective (thermal) mass, so that the equations for quark and hole can be solved simultaneously following [35];

$$[(\epsilon - V(r))^2 - \mu^2 - \hat{p}^2] \psi(r) = 0 \quad (12)$$

where \hat{p} is momentum operator, and the reduced energy and mass are $\epsilon = (E^2 - m_1^2 - m_2^2)/2E$, $\mu = m_1 m_2 / E$ with $m_1 = m_2 = m_q$.

Furthermore from eq.(9),

$$\langle \vec{\alpha} \rangle = (\Psi^\dagger, \vec{\sigma} \Phi) + (\Phi^\dagger, \vec{\sigma} \Psi) = \frac{\vec{p}}{p_0} - \frac{i}{p_0} \langle [\vec{\sigma} \times \vec{p}] \rangle. \quad (13)$$

If $\vec{\sigma}$ is parallel to \vec{p} , as in states of good helicity, the second term does not contribute. From the chirally restored Dirac equation (8), ignoring spin effects such as the spin-orbit interaction which is zero in S-states we are considering, we find $p_0^2 = \vec{p}^2$.

Brown [36] showed that in a stationary state the EM interaction Hamiltonian between fermions is

$$H_{\text{int}} = \frac{e^2}{r} (1 - \vec{\alpha}_1 \cdot \vec{\alpha}_2), \quad (14)$$

where the $\vec{\alpha}_{1,2}$ are the velocities. Applying (14) to the chirally restored domain of QCD, we expect

$$\begin{aligned} H_{\text{int}} &= \frac{2\alpha_s}{r} && \text{for } \vec{\alpha}_1 \cdot \vec{\alpha}_2 = -1 \\ &= 0 && \text{for } \vec{\alpha}_1 \cdot \vec{\alpha}_2 = +1 \end{aligned} \quad (15)$$

2.2 The spin-spin interaction

The nonrelativistic form of the spin-spin interaction, in the delta-function form, may give an impression that it is maximal at the smallest distances. However this is not true, as becomes clear if the relativistic motion is included in full, and in fact at $r \rightarrow 0$ it is suppressed. At large r , when particle motion is slow, it is of course again suppressed, thus contributing mostly at some intermediate distances.

This fact is clear already from the derivation of the 1s-state hyperfine splitting Fermi-Breit due to hyperfine interaction in hydrogen from 1930 [37] given by

$$\delta H = \frac{2}{3}(\vec{\sigma} \cdot \vec{\mu}) \int d^3r \frac{\psi^\dagger \psi}{r^2} \frac{d}{dr} \frac{e}{E + e^2/r + m} \quad (16)$$

Note the complete denominator, which non-relativistically is just substituted by m alone, but in fact contains the potential and is singular at $r \rightarrow 0$. The derivative of the e^2/r in the denominator insured that the electric field was zero at $r = 0$. Here $\vec{\sigma}$ is the electron spin, $\vec{\mu}$ the proton magnetic moment. In eq (16) the derivative can then be turned around to act on $\psi^\dagger \psi$, and to order $\alpha = 1$ and with the e^2/r neglected in the denominator, one has

$$\delta H \simeq -\frac{8\pi}{3}(\vec{\sigma} \cdot \vec{\mu}) \frac{e}{2m} \psi^2(0), \quad (17)$$

with ψ taken to be the nonrelativistic $1s$ wave function to lowest order in α .

The hyperfine structure is obtained by letting the first \vec{p} in eq. (10) act on the p_0^{-1} and the second \vec{p} go $\vec{p} + \sqrt{\alpha_s} \vec{A}$ with

$$\vec{A} = \frac{\vec{\mu} \times \vec{r}}{r^3} \quad (18)$$

with $\vec{\mu}$ the magnetic moment of the anti-quark. One finds that the hyperfine structure is [37]

$$H_{\text{hfs}} = \frac{1}{p_0^2} \sqrt{\alpha_s} \vec{\sigma} \cdot [\vec{E} \times \vec{A}] \quad (19)$$

where \vec{E} is the color electric field. Thus,

$$H_{\text{hfs}} = \frac{\sqrt{\alpha_s} |\vec{E}|}{p_0^2} \left(\frac{\vec{\sigma} \cdot \vec{\mu}}{r^2} - \frac{\vec{\sigma} \cdot \vec{r} \vec{\mu} \cdot \vec{r}}{r^4} \right) = \frac{2}{3} \frac{\sqrt{\alpha_s} |\vec{E}|}{p_0^2} \frac{\vec{\sigma} \cdot \vec{\mu}}{r^2}. \quad (20)$$

where $|\vec{E}| = 2\alpha_s/r^2$. As in the hydrogen atom, the magnetic moments of quarks and anti-quarks are

$$\mu_{q,\bar{q}} = \mp \frac{\sqrt{\alpha_s}}{p_0 + m_{q,\bar{q}}} \quad (21)$$

except that the Dirac mass $m_{q,\bar{q}} = 0$ and p_0 , in which the potential is increased by a factor of 2 to take into account the velocity-velocity interaction, is now

$$p_0 = E + 2(\alpha_s/r) \quad (22)$$

for QCD so that in terms of the quark and anti-quark magnetic moment operators ¹⁴,

$$H_{\text{hfs}} = -\frac{2}{3} \frac{|\vec{E}|}{p_0 r^2} (\vec{\mu}_q \cdot \vec{\mu}_{\bar{q}}). \quad (23)$$

Of course, our p_0 for the chirally restored regime has substantial r dependence (whereas the e/r in the hydrogen atom is generally neglected, and $E + m$ is taken to be $2m$, so that $\mu_e = -e/2m_e$). From Fig. 3 it will be seen that (square of) the wave function is large just where α_s/r is large.

For rough estimates we use averages. We see that, as in Table 1, if E is to be brought down by $\sim 0.5m_q$ for the σ and π by the Coulomb interaction, then

$$2\langle\alpha_s/r\rangle \simeq \frac{1}{2}m_q \simeq \frac{1}{4}p_0 \quad (24)$$

so that with $\alpha_s \sim 0.5$,

$$\langle r^{-1} \rangle \simeq \frac{1}{2}m_q. \quad (25)$$

We next see that this is consistent with the spin splitting forming a fine structure of the two groups, the lower lying σ and π , and the slightly higher lying vectors and axial vectors. Using our above estimates, we obtain

$$\langle H_{\text{hfs}} \rangle \simeq \frac{1}{24} \frac{1}{16} \vec{\sigma}_q \cdot \vec{\sigma}_{\bar{q}} m_q, \quad (26)$$

so that for the σ and π where $\vec{\sigma}_1 \cdot \vec{\sigma}_2 = -3$ we have

$$\langle H_{\text{hfs}} \rangle \sim -\frac{m_q}{128}, \quad (27)$$

the approximate equality holding when $\alpha_s = 0.5$. Note that the hyperfine effect is negligible for the $\alpha_s \sim 0.5$. Although formally eq. (26) looks like the hyperfine structure in the chirally broken sector, it is really completely different in makeup.

In our expression for $\langle H_{\text{hfs}} \rangle$ we have the r dependence as $(p_0 r)^{-4} r^{-1}$ and $p_0 r = 4$, basically because the Coulomb interaction lowers the π and σ only

¹⁴ The electric field is denoted as \vec{E} which should be distinguished from the energy E .

1/4 of the way to zero mass. This explains most of the smallness of the spin-dependent interaction.

A recently renewed discussion of spin-spin and spin-orbit interactions in a relativistic bound states has been made Shuryak and Zahed [38], who derived their form for both weak and strong coupling limits. Curiously enough, the spin-spin term changes sign between these two limits: perhaps this is another reason why at intermediate coupling considered in this work it happens to be so small.

2.3 The effect of the instanton molecules

The effective interaction is calculated as follows. The propagator is written as

$$S(x, y) = \sum_{\lambda} \frac{\phi_{\lambda}^{\dagger}(x)\phi_{\lambda}(y)}{\lambda + im} \quad (28)$$

where λ, ϕ_{λ} are eigenvalues and eigenfunctions of the Dirac operator. If the gauge field configuration is the anti-instanton-instanton ($\bar{I}I$) molecule, the 2 lowest eigenvalues are $\lambda = \pm|T_{\bar{I}I}|$ and their eigenfunctions are simple combinations of zero modes for instanton and anti-instanton $\phi_I \pm \phi_{\bar{I}}$. The sum of those leads to

$$S(x, y) = \frac{2}{|T_{\bar{I}I}|}(\phi_I^{\dagger}(x)\phi_{\bar{I}}(y) + \phi_{\bar{I}}^{\dagger}(x)\phi_I(y)) \quad (29)$$

This can be interpreted as follows: $\phi_I(x)$ is the amplitude to go from point x to the instanton I , the other phi is the amplitude to appear from the anti-instanton, and the factor in front is the propagator between I and \bar{I} .

For propagation of 2 quarks, say of opposite flavors, one can then draw the two diagrams shown in Fig.1. The diagram (a) read from left to right has quarks of opposite chirality, so it contributes to scalar and pseudoscalar mesons; the diagram (b) has the same chirality of quark and anti-quark, so it contributes to vector and axial vector channels. One can see from the figure that in the former case both $\bar{q}q$ go into the same instanton, while in the latter they have to go to the opposite ones. As a result, the locality of the former vertex is given by the instanton size ρ and of the latter by the size of the molecule.

If all 4 points are far from the instanton and anti-instanton, $\phi(x) \sim 1/x^3$ modulo a constant spinor. This power of the distance corresponds to free propagator for a massless quark, $S_0 = 1/(2\pi^2 x^3)$, which should be “amputated”,

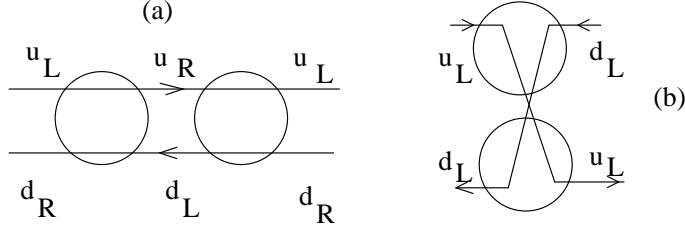


Fig. 1. The diagrams generating the effective Lagrangian

leading to a constant vertex function, or effective Lagrangian [25]. The effective interaction between quarks is conveniently calculated by rearranging the exchange terms into a direct interaction. The resulting Fierz symmetric Lagrangian reads [25]

$$L_{mol\,sym} = G \left\{ \left[(\bar{\psi} \tau^a \psi)^2 - (\bar{\psi} \tau^a \gamma_5 \psi)^2 \right] - \frac{1}{4} \left[(\bar{\psi} \tau^a \gamma_\mu \psi)^2 + (\bar{\psi} \tau^a \gamma_\mu \gamma_5 \psi)^2 \right] + (\bar{\psi} \gamma_\mu \gamma_5 \psi)^2 \right\} + L_8, \quad (30)$$

with the last complicated term containing color-octet $\bar{q}q$ pairs only. The coupling constant is now proportional to the density of molecules

$$G = \frac{2}{N_c^2} \int n(\rho_1, \rho_2) d\rho_1 d\rho_2 \frac{1}{8T_{IA}^2} (2\pi\rho_1)^2 (2\pi\rho_2)^2. \quad (31)$$

If the molecules are incompletely polarized in the (Euclidean) time direction then all vector terms are modified accordingly, because $(\bar{\psi} \gamma_\mu \Gamma \psi) \sim \bar{z}_\mu$, the only vector available.

We start by explaining the issue of the “polarization” of the $\bar{I}I$ molecules. Let us put I at the origin and in the standard SU(3) orientation without rotation. Let us introduce the 4-d polar angle θ_4 : the position vector of \bar{I} , called \bar{z}_μ is such that $\bar{z}_4 = \cos(\theta_4) \sqrt{\bar{z}_\mu^2}$. We will refer to the $\theta_4 = 0$ case as molecules completely polarized in the time direction: as discussed in [25] this is where the maximum of the Z is. The very robust maximum corresponds to “half Matsubara box”, $\bar{z}_4 = 1/(2T)$, and if θ_4 is nonzero Z is smaller, basically because of large distances in the $T_{\bar{I}I}$. Let us estimate the effect of that, ignoring the gauge action,

$$Z \sim |T_{\bar{I}I}|^{2N_f} \sim \left(\frac{1}{(2T \cos(\theta_4))^{-2} + \rho^2} \right)^{2N_f} \quad (32)$$

which can be expanded into Gaussian form at small θ_4 . For 2 flavors and $T = T_c \approx 1/(4\rho)$, the root mean square polarization angle is $\langle \theta_4 \rangle \approx 0.55$. We will need below

$$\cos^2(\langle\theta_4\rangle) \approx .72 \quad \sin^2(\langle\theta_4\rangle) \approx .28 \quad (33)$$

corresponding to $\langle\theta_4\rangle = 32^\circ$.

Let us remember that for vector particles propagating in matter one can define in general 2 structures in the polarization operator, the longitudinal and transverse ones $\Pi_{L,T}$, which are related to 1 longitudinal and 2 transverse modes. Those are related to Cartesian components as follows

$$\Pi_{00} = \Pi_L, \quad \Pi_{0n} = \frac{\omega p_n}{\vec{p}^2} \Pi_L \quad (34)$$

$$\Pi_{mn} = \left(\delta_{mn} - \frac{p_m p_n}{\vec{p}^2} \right) \Pi_T + \frac{\omega^2 p_m p_n}{\vec{p}^2} \Pi_L \quad (35)$$

where the Latin indices are 1-3 and Greek 0-3, $\omega = p_0$. This polarization tensor satisfies the conservation law $p_\mu \Pi_{\mu\nu}$, eliminating the 4-th component.

For complete polarization of molecules, $\theta_4 = 0$ and only the zeroth component (the longitudinal Π_L component) is coupled, while in general the coefficients include \sin^2 and \cos^2 of the angles determined above (33) in Π_T and Π_L , respectively.

This results in additional nonlocal correction factors, which for the scalar-pseudoscalar channels is

$$F_{nonlocal}^{S,PS} = \left| \int d^4x \frac{\chi(x)}{\chi(0)} |\phi_I(x)|^2 \right|^2 \quad (36)$$

and for the vector-axial-vector ones

$$F_{nonlocal}^{V,A} = \left\langle \left| \int d^4x \frac{\chi(x)}{\chi(0)} \phi_I(x) \phi_{\bar{I}}(x) \right|^2 \right\rangle_{\theta_4} \quad (37)$$

where the additional angular bracket in the latter case comes about from averaging over the molecular orientation relative to the time axes. Note that in the former case, as well as in the latter for $\theta_4 = 0$, the correction factors are 1, due to the normalization condition $\int d^4x |\phi_I(x)|^2 = 1$, for weakly bound (large size) states, for which the factor $\chi(x)/\chi(0)$ can be approximated by 1 and taken out of the integral. We treat the ratios $(\chi(x)/\chi(0))^2 = F$ as a vertex correction in our calculations in the next section, and estimate their size in the Appendix.

The effective interaction of light quarks, the Fierz symmetric instanton molecule Lagrangian of Schäfer et al.[25] in Minkowski space, is of the form

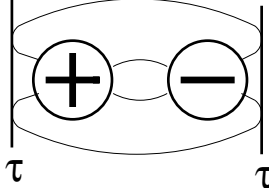


Fig. 2. Looking down on the instanton molecule close-packed around the antiperiodic time direction at T_c . Here ρ is the $\frac{1}{3}$ fm radius of the instanton or anti-instanton and $\tau = 1/4\rho \sim 150$ MeV. Just at T_c the instanton molecule is fully polarized in the τ direction. The lines going in and out of the instanton and anti-instanton are the quark zero modes. The outer quark zero modes are broken open to give the quark-quark interaction which forms the instanton induced interaction.

$$L_{IML} = G \left\{ (\bar{\psi} \tau^\alpha \psi)^2 + (\bar{\psi} \tau^\alpha \gamma_5 \psi)^2 + \frac{1}{4} [(\bar{\psi} \tau^\alpha \gamma_\mu \psi)^2 - (\bar{\psi} \tau^\alpha \gamma_\mu \gamma_5 \psi)^2] - (\bar{\psi} \gamma_\mu \gamma_5 \psi)^2 \right\}. \quad (38)$$

The value of G at T_c was obtained by BGLR [17] as

$$G = 3.83 \text{ GeV}^{-2}. \quad (39)$$

Here $\tau^\alpha = (\tau, 1)$ is a four-component vector. This Lagrangian gives attraction in the $\sigma, \delta, \pi, \rho$ and A_1 sectors. We will find that the mesons are bound by both the color Coulomb and the four-Fermi instanton molecule interactions.¹⁵

We should explain how the chirally broken NJL is relayed into the chirally restored NJL as T goes upwards through T_c . The 't Hooft instanton-driven interaction has been included in the chirally broken NJL, and undoubtedly enters into the interactions which bring the m_π to zero and the m_σ to $2m_q$, although their role relative to the other interactions is not clear in this domain. As noted in BGLR[17], about half of the total bag constant (conformal anomaly) coming from the spontaneous breaking of chiral symmetry (the restoration of which is associated with Brown/Rho scaling) is transferred from that of the binding energy of the negative energy nucleons, which are the relevant $T = 0, \rho = 0$ variables to the rearrangement of the random instanton vacuum into the instanton molecules (which do not break chiral symmetry) and the other half goes into melting the soft glue as the nucleons loosen into constituent quarks.

BGLR[17] showed that NJL could be continued from the chirally broken region

¹⁵ As often the case in condensed matter and particle physics, attractive four-Fermi interactions could – via anomalous dimensions – figure crucially in phase transitions, so may play a more important role near T_c . This may be particularly relevant to other mesons than the π and σ . It is shown in [22] with a schematic model that the vector mesons do undergo a phase change very similar to that of the π and σ .

up to the chirally restored one with the $\sim 6\%$ decrease in the NJL coupling

$$\begin{aligned} G = 4.08 \text{ GeV}^{-2} & \quad \text{chirally broken phase} \\ G = 3.83 \text{ GeV}^{-2} & \quad \text{chirally restored phase.} \end{aligned} \quad (40)$$

We suggest that the fragility of chiral symmetry breaking as T moves upwards to T_c signifies the importance of the instanton molecules in this region of T . With only an $\sim 6\%$ decrease in G , the chiral restoration transition is effectuated.

Whereas in the chirally broken NJL, the vector interactions are about the same size as the scalar ones, one can see from the instanton molecule Lagrangian, eq. (38), that the ρ and A_1 interactions are a factor of 4 smaller than the π and σ ones. However, as we have outlined, taking the instanton molecule to be polarized along the time axis, the time components of ρ and A_1 interactions are built up a factor of 4, at the expense of the spatial ones. Thus, in the classical approximation, neglecting fluctuations in θ_4 , the vector and axial vector modes would be degenerate with σ and π .

For the local 4-fermion interaction with the coupling constant G the energy shift is given simply by

$$\delta E = G|\psi(0)|^2 \quad (41)$$

More generally, for the non-local interaction induced by molecules, one should project on the (2-body) wave function of the bound state $\Psi(x, y) = \exp[iP_\mu(x+y)_\mu/2]\chi(x-y)$ where, for the stationary state, there is no dependence on relative time $x_0 - y_0$.

The interaction is attractive in all channels, so that if the Coulomb interaction does not bring the meson mass all the way to zero, the instanton molecule interactions will, in particular near the phase transition temperature T_c , where the wave functions are very compact.

In the NJL-like instanton molecule Lagrangian eq. (38) the interactions are four-point in nature. We can convert these to an instanton molecule interaction by constructing a pseudo-potential $V = C\delta(x)$ for the $\bar{\psi}\psi \rightarrow \bar{\psi}\psi$ scattering amplitude. Here $\langle \bar{\psi}\delta(x)\psi \rangle = \bar{\psi}\psi(0)$. Therefore $C = G\bar{\psi}\psi(0)$ with G the interaction of eq. (39), gives the strength of the pseudo-potential.

Let us mention some estimates for the mass of the vector/axial mesons. Keeping as above the thermal quark mass at $m_q = 1\text{GeV}$ and the $\alpha_s = 0.5$ results from Table 1, we will see that the Coulomb binding of ~ 0.5 GeV plus that

due to instanton molecules ~ 1 GeV is able to make π, σ mesons massless, once we sum loops.

In the Appendix we estimated that the corrections for nonlocality were roughly equal for π, σ and ρ, A_1 , so that the masses of the latter scale as $\cos^2(\langle\theta_4\rangle)$ and $\sin^2(\langle\theta_4\rangle)$ relative to the $2m_q \simeq 2$ GeV binding energy of the π and σ . From our estimates Eq. (33) we see that the (predominantly) longitudinal ρ, A_1 masses will come at ~ 560 MeV and the transverse ρ, A masses at 1440 MeV; i.e., at roughly the free ρ and A_1 masses, respectively. However, the quasiparticle composed of coupled ρ and 2π components (“rhosobar”) may lie lower in energy when the interaction is diagonalized.

2.4 The resulting $\bar{q}q$ binding

We first construct the bound states for $T \gtrsim T_c$ (*unquenched*), at temperature close enough to T_c so that we can take the running coupling constants at $T = T_c + \epsilon$. The fact that we are above T_c is important, because the $\Lambda_{\chi\text{SB}} \sim 4\pi f_\pi \sim 1$ GeV which characterizes the broken symmetry state below T_c no longer sets the scale. Until we discover the relevant variables above T_c we are unable to find the scale that sets $\alpha_s = \frac{4g^2}{3\hbar}$, the color Coulomb coupling constant.

Following SZ [11], we adopt quark-anti-quark bound states to give the relevant unperturbed representation and, the instanton molecule gas [25] as a convenient framework. In particular, Adami et al.[39], Koch and Brown[40], and BGLR [17] have shown that $\gtrsim 50\%$ of the gluon condensate is not melted at $T = T_c$. The assumption motivated by Ilgenfritz & Shuryak [16] is then that the glue that is left rearranges itself into gluon molecules around $T = T_c$, i.e., what BGLR call “epoxy”. We have quantitatively determined couplings for the mesons in the instanton molecule gas by extending the lower energy NJL in the chiral symmetry breaking region up through T_c [17]. We set these couplings in order to fit Miller’s [41] lattice gauge results for the melting of the soft glue.

In Fig. 3 we show that if we choose $\alpha_s = 1$ (effectively $\alpha_s = 2$ by the doubling in Eq. (15)) as would be required to enter the strong coupling region considered by Shuryak and Zahed[14] we bring the meson mass down by $-1.36 m_q$ from their unperturbed $2 m_q$. However, we switch to the region of $\alpha_s \sim 0.5$, which is required by charmonium (intermediate coupling). In Table 1 we summarize the Coulomb binding for a few choices of α_s .

In the case of the instanton molecule interaction the coupling constant $G = 3.83 \text{ GeV}^{-2}$ is dimensionful, so that its contribution to the molecule energy scales as $G m_q^3$. (Since we take $\alpha_s = 0.5$ and will find that with inclusion of

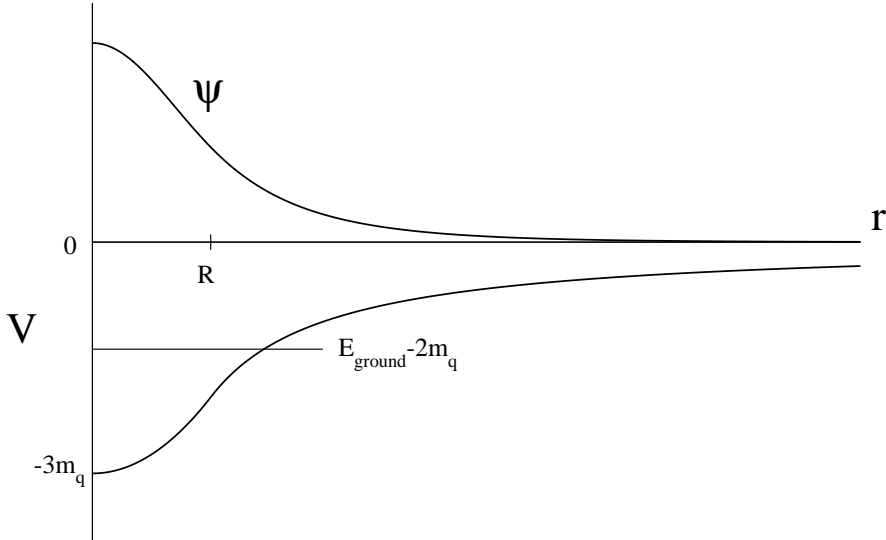


Fig. 3. The color Coulomb potential V and the corresponding wave function ψ for relativistic Klein-Gordon case. The interaction eq. (7) with $R = \hbar/2m_q$ was used. The ground state energy with $\alpha_s = 1$ corresponds to $E_{\text{ground}} = 0.645 m_q$. The minimum of the potential at the origin is at $-3m_q$ here.

the velocity-velocity interaction the effective α_s will be 1, powers of α will not affect our answer. We will use $m_q = 1$ GeV, essentially the lattice result for $\frac{3}{2}T_c$ and $3T_c$ [13], which works well in our schematic model.) Of course, in QCD the Polyakov line goes to zero at T_c , indicating an infinite quark mass below T_c ; i.e., confinement. Just at T_c the logarithmically increasing confinement force will not play much of a role because the dynamic confinement holds the meson size to $\sim \hbar/m_q c$, or ~ 0.2 fm with our assumption of $m_q = 1$ GeV. (Later we shall see that the rms radius is ~ 0.3 fm.) Since we normalize the instanton molecule force, extrapolating it through T_c (unquenched), and obtain the color Coulomb force from charmonium, our m_q is pretty well determined. However, our $m_q = 1$ GeV is for the unquenched system and at a temperature where the instanton molecules play an important role.

Given these caveats, we may still try to compare our Coulomb result with the lowest peak of Asakawa et al.[42] which is at ~ 2 GeV for $T = 1.4T_c \sim 0.38$ GeV and for Petreczky at $\lesssim 5T \sim 2.030$ GeV for $T = 1.5T_c \sim 0.406$ GeV where we used the Asakawa et al. T_c (quenched). We wish to note that: (i) These temperatures are in the region of temperatures estimated to be reached at RHIC, just following the color glass phase (which is estimated to last $\sim 1/3$ fm/c). Indeed, Kolb et al. begin hydrodynamics at $T = 360$ MeV. (ii) These

| α_s | $\Delta E_{\text{Coulomb}}$ [GeV] | $\sqrt{\langle r^2 \rangle}$ [fm] | $\Delta E_{\text{4-point}}$ [GeV] |
|------------|-----------------------------------|-----------------------------------|-----------------------------------|
| 0.50 | -0.48 | 0.36 | -0.99 |
| 0.55 | -0.60 | 0.31 | -1.39 |
| 0.60 | -0.71 | 0.28 | -1.83 |
| 1.00 | -1.36 | 0.14 | -7.57 |

Table 1

Binding energies from color Coulomb interaction and the corresponding rms radii for various α_s (effectively, $2\alpha_s$ including velocity-velocity interaction). 4-point interactions are calculated using the parameters obtained from color Coulomb interaction.

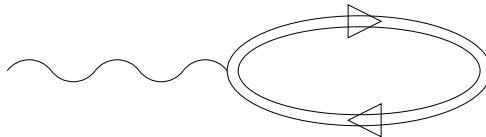


Fig. 4. Coulomb molecule. The wavy line on the left represents the momentum transfer necessary to produce the molecule. The double line denotes the Furry representation, i.e., the full propagator in the Coulomb potential.

are in the region of temperatures estimated by SZ[11] to be those for which bound mesons form.

We are unable to extend our consideration to higher temperatures, where the situation may move towards the perturbative one, but we believe that lattice calculations do support our scenario that the QGP contains large component of bound mesons from $T \sim 170$ MeV up to $T \sim 400$ MeV.

For $\alpha_s = 0.5$, which is the value required to bind charmonium up through $T = 1.6T_c$, we find that the Coulomb interaction binds the molecule by ~ 0.5 GeV, the instanton molecule interaction by ~ 1.5 GeV. However, the finite size of the $\psi^\dagger\psi$ of the instanton zero mode could cut the latter down by an estimated $\sim 50\%$ (See Appendix). As in the usual NJL, there will be higher order bubbles, which couple the Coulomb and instanton molecule effects.¹⁶ We draw the Coulomb molecule in Fig. 4, where the double lines denote the Furry representation (Coulomb eigenfunction for quark and anti-quark in the molecule).

The four-point instanton molecule interaction is shown in Fig. 5. There will be higher-order effects as shown in Fig. 6, of the 4-point interaction used in higher-order between Coulomb eigenstates which always end in a 4-point interaction. The energy of the propagators has been lowered from the 2 GeV

¹⁶ Alternatively, the δ -function of the 4-point interaction should be included in the Klein-Gordon equation, where it will change the energy.

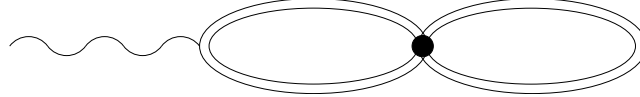


Fig. 5. The four-point instanton molecule interaction between Coulomb eigenstates. The $(\bar{\psi}\psi)^2$ intersect at the thick point.

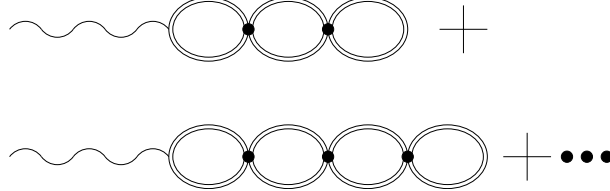


Fig. 6. Higher order effects of four-point interaction.

of the two noninteracting quarks to 1.5 GeV by the Coulomb interaction. The series beginning with terms in Figs. 4–6 is

$$\begin{aligned}\Delta E &= -0.5\text{GeV} - 1\text{GeV } F - \frac{1(\text{GeV})^2 F^2}{1.5\text{GeV}} - \frac{1(\text{GeV})^3 F^3}{(1.5\text{GeV})^2} + \dots \\ &= -0.5\text{GeV} - \frac{1\text{GeV} F}{1 - \frac{1\text{GeV} F}{1.5\text{GeV}}}.\end{aligned}\quad (42)$$

Now $\Delta E = -1.25$ GeV is accomplished for $F = 0.5$, a reasonable assumption from the estimate in the Appendix.

Working in the Furry representation (including the Coulomb potential exactly), we have a -0.5 GeV shift already from the Coulomb wave functions. This means that we must obtain $\Delta E = -1.5$ GeV to compensate for the $2m_q = 2$ GeV, in order to bring the π and σ masses to zero. The four-point interaction is a constant, at a given temperature, so this problem is just the extended schematic model of nuclear vibrations (See Sec. V of Brown [44], where simple analytical solutions are given).

Our eq. (42) corresponds to the Tamm-Dancoff solution, summing loops going only forward in time. If ΔE decreases -0.75 GeV in this approximation, then when backward going graphs are added, then ΔE will decrease by twice this amount [44], or the -1.5 GeV necessary to bring the π and σ energy to zero. (There is an analogy between the treatment of the spurion and the Goldstone mode in hadronic physics.) Of course, forward and backward going loops are summed in the Bethe-Salpeter equation to give the NJL in the broken symmetry sector, but the actual summation is more complicated there, because the intermediate state energies are not degenerate.

In detail, with our estimated $F = (0.75)^2$ from the Appendix and the 4-point energies from Table 1, our π and σ excitations without inclusion of backwards going graphs are brought down 58% of the way from -0.5 GeV to -2 GeV;

i.e., slightly too far. We have not made the adjustment down to 50%, because the uncertainties in our estimate of F , etc., do not warrant greater accuracy.

2.5 Comparison with Lattice Calculations

Lattice calculations propagating quarks and anti-quarks in the spatial direction gave evidence of DeTar's dynamical confinement [45]. The dynamical confinement comes about from the attractive $\alpha_s \vec{\alpha}_1 \cdot \vec{\alpha}_2 / r$, or current-current interaction in our eq. (14). This is the same in the “funny space”, since the x and y directions, in which the current loops lie, are as in the real space. Thus we find from eq. (14) that the introduction of the Coulomb interaction doubles the effects from the current-current interaction. The instanton molecule interaction gives a factor of several times the current-current interaction. It should be included in the unquenched lattice calculations.

It is instructive to examine the results of Bernard et al.[45] (reproduced in Fig.8.6 of Adami and Brown [46]) for two-dimensional wave functions at $T = 210$ and $T = 350$ MeV of the chirally restored π and ρ . These wave functions are given in physical units. They have been measured on the (x, y) -plane and we think of them as projections onto this plane of the three-dimensional wave function. The pion wave function at $T = 210$ MeV is seen to drop off exponentially, decreasing to 0.02 of its $r = 0$ value by $r = 1.15$ fm. With a wave function $C \exp(-\kappa r)$, this indicates a κ of $3.4 \text{ fm}^{-1} = 0.68 \text{ GeV}$. This gives an rms radius for the two-dimensional wave function of $\sqrt{6}/2\kappa = 1.8 \text{ GeV}^{-1} = 0.36 \text{ fm}$. For the three-dimensional one we would multiply by $\sqrt{3/2} \simeq 1.22$; thus one arrives at an rms radius of $\sim 0.44 \text{ fm}$. This is not much larger than the 0.36 fm for our chosen $\alpha = 0.5$, and it should not be because of the relatively small role played by the Coulomb term.

It can be seen that the ρ -meson wave function does not drop exponentially until $2 - 3$ fm, showing it to be larger in extent than the pion. It then appears to decrease somewhat more slowly than the pion wave function, although the errors are such that there is uncertainty in this. The true quasiparticle above T_c may, however, be a linear combination of ρ and 2 pion states.

The instanton molecule model, as the DeTar dynamical confinement, involves an analytical continuation from imaginary to real time, although it is quite simple in the former. The SZ [11] Coulomb-bound gas of mesons is formulated directly in real time. It is simple and straightforward. We view it to be useful to give our alternative instanton molecule formulation, because it enables us to make contact with the lattice calculation, especially with those of the gluon condensate.

Hadronic spectral functions above the QCD phase transition have been calculated in quenched lattice gauge simulations by Asakawa, Hatsuda, & Nakahara [42] and by Petreczky [43].

In the quenched approximation, the wavy line in Fig. 4 can be interpreted as the source current which creates a valence quark and anti-quark. These are allowed to exchange any number of gluons, so it is appropriate to let them exchange any number of Coulomb interactions, as well as develop thermal masses; i.e., the Coulomb problem is that which we outlined.

We differ in detail from SZ[11], in that we consider the 32 normal modes of $\bar{q}q$ states, in which the quark and anti-quark, or quark and hole, have opposite helicities so as to benefit from the current-current interaction. SZ have the bound states of quark and anti-quark, or quark and hole, and, separately, those of gluons, the glueballs. Because of the larger Casimir operator for the gluons, these bind at a higher temperature than the quarks, so there would be two regions of temperature in which the molecules break up. The number of degrees of freedom, 40 quarks and 16 gluons, once they break up, would be different. Presumably they would have the same $q\bar{q}$ bound states for $T \sim T_c$ as we, but, in addition, would have the glueballs.

As noted by SZ, in the region where the molecules break up, the quark velocities are small, going to zero at zero binding energy. This means that the velocity-velocity interaction will be unimportant and the additional 32 degrees of freedom, disfavored at lower temperatures by the velocity-velocity interaction, will become important, doubling the degrees of freedom.

However, the quenched approximation would not include the quark and anti-quark loops of the instanton molecule interaction. Thus, at $T = T_c$ we would have molecules of energy 1.5 GeV, since our Coulomb interaction gives a 0.5 MeV binding on thermal quark and anti-quark masses, each of 1 GeV. (In fact, these masses were measured at $1.5T_c$ (*quenched*), and need not be the same at T_c . Furthermore, we need to mention that our T_c is that for the unquenched calculations, $T_c = 170 - 175$ MeV, because we necessarily have a situation with quarks and anti-quarks, especially instanton zero modes.)

In Fig. 7 we show Asakawa & Hatsuda[6] spectral functions for (quenched) temperatures of $1.4T_c \sim 380$ MeV and $1.9T_c \sim 515$ MeV. The lower temperature is essentially that reached at RHIC following the color glass phase and the second temperature is higher, but probably not in the perturbative regime because the lattice calculations by Petreczky et al.[13] give the quark mass at $3T_c$ as roughly the same as at $\frac{3}{2}T_c$, not increasing as gT .

The narrow 2 GeV peak supports our identification of this temperature ($T \sim 380$ MeV) being where the molecules break up, because the particle velocities

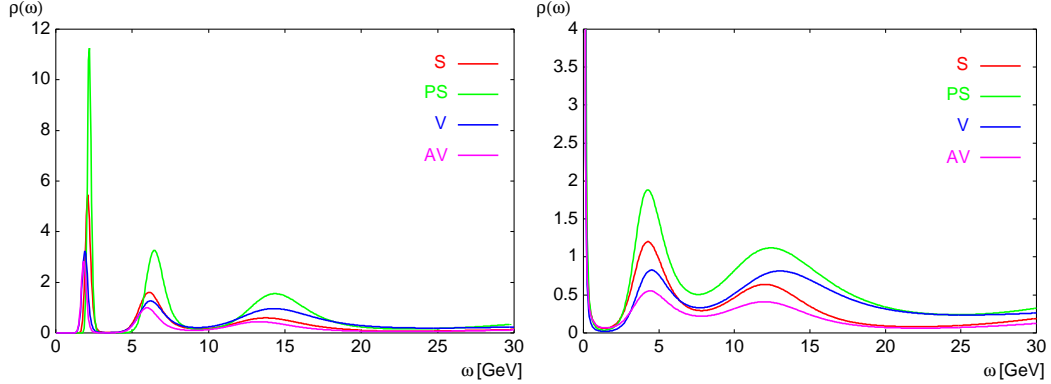


Fig. 7. Spectral functions of Asakawa et al.[42]. Left panel: for $N_\tau = 54$ ($T \simeq 1.4T_c$). Right panel: for $N_\tau = 40$ ($T \simeq 1.9T_c$).

will begin from zero at breakup.¹⁷ In this case, the 2 GeV reproduces the sum of quark and anti-quark masses. We note the meson degeneracy is consistent with our negligible effects from spin and chiral restoration of the π and σ and vector and axial vectors.

The $1.9T_c \sim 515$ MeV data which should be well above the temperature at which the molecules break up does show definite thermal effects. As noted earlier, the lattice calculations give approximately the same m_q at $3T_c$ as at $(3/2)T_c$, so we can take m_q to be constant in this region of energies. Each of the ~ 1 GeV quark and hole in quark and anti-quark will have a thermal energy of ~ 1.1 GeV, midway between the $\frac{3}{2}T$ nonrelativistic thermal energy and the $3T$ relativistic one. Therefore, it costs ~ 4.2 GeV to produce a quark particle and hole or quark and anti-quark at this temperature. The half width of the peak is roughly consistent with the size of the proposed thermal energy.

At low ω we probably see Landau damping in the $1.9T_c$ results, although at $1.4T_c$ there is no such sign. This further supports our belief that the quark and anti-quarks are essentially at rest there.

By rescaling the lattice calculation Peter Petreczky (private communication) has shown that the peaks higher than the first one are lattice artifact.

We see that in the SZ[11] model, one can understand not only in general terms, but also many of the details of the Asakawa and Hatsuda lattice calculations.

¹⁷ In the LGS the zero-momentum state of the quark-anti-quark pair is projected out.

3 Conclusions

Shuryak and Zahed have discussed the formation of the mesonic bound states at higher temperatures, well above T_c . They pointed out that in the formation of the bound state, or any one of the molecular excited states, the quark-quark scattering length becomes infinite, similarly for the more strongly bound gluon-gluon states. In this way the nearly instantaneous equilibration found by RHIC can be explained. As we explained in the last section, lattice calculations seem to support the scenario of nearly bound scalar, pseudoscalar, vector and axial-vector excitations at $\sim 2T_c$ (*unquenched*) (~ 1.5 times the quenched T_c).

In this work we are able to construct a smooth transition from the chirally broken to the chirally restored sector in terms of continuity in the masses of the σ and π mesons, vanishing at $T \rightarrow T_c$. In doing so we had to include relativistic effects. One of them – the velocity-velocity term related to Ampere law for the interacting currents – nearly doubles the effective coupling. The spin-spin term happens to be very small. The crucial part of strong binding in our picture of $\bar{q}q$ mesons (or molecules) is the quasi-local interaction due to instanton molecules (the “hard glue”). We found that the tight binding of these mesons near T_c enhances the wave function at the origin, and gives us additional understanding of the nonperturbative hard glue (epoxy) which is preserved at $T > T_c$.

Thus, we believe that the material formed in RHIC was at a temperature where most of it is made of chirally restored mesons. Certainly this is not the weakly coupled quark-gluon plasma expected at high T .

Finally, in this paper we have focused on quantum mechanical binding effects in the vicinity of the critical temperature T_c coming down from above. Nice continuity in the spectra of the light-quark hadrons – e.g., the pions and the σ – across the phase boundary should also hold for other excitations such as the vector mesons ρ, ω, A_1 which lie slightly above π and σ because of quantum corrections. Since going below T_c from above involves a symmetry change from Wigner-Weyl to Nambu-Goldstone, there is a phase transition and to address this issue, it would be necessary to treat the four-fermi interactions more carefully than in the pseudo-potential approximation adopted here. As briefly noted, the true quasiparticles in the ρ -channel in the many-body medium may be linear combinations of the ρ found here and 2π states.

Acknowledgments

We would like to thank Santo Fortunato, Peter Kolb, Peter Petreczky, Madappa Prakash and Ismail Zahed for many extremely useful discussions. GEB and ES were partially supported by the US Department of Energy under Grant No. DE-FG02-88ER40388. CHL is supported by Korea Research Foundation Grant (KRF-2002-070-C00027).

A Appendix: Finite Size Corrections

The instanton is $\sim 1/3$ fm in radius, and the rms radius of the molecule is about the same for $\alpha_s = 0.5$, so there will be a correction for the finite size of the instanton zero modes. Their wave functions are

$$\psi_{ZM} = \frac{\rho/2\pi}{(x^2 + \rho^2)^{3/2}} \quad (\text{A.1})$$

with ρ the instanton radius. Now

$$\bar{\psi}\psi \propto \frac{1}{(x^2 + \rho^2)^3}. \quad (\text{A.2})$$

Integrating over time

$$\begin{aligned} \int d\tau \frac{1}{(x^2 + \rho^2)^3} &\sim \frac{1}{(r^2 + \rho^2)^{5/2}} \propto \exp \left[-\frac{5}{2} \ln \left(\frac{r^2}{\rho^2} + 1 \right) \right] \\ &\approx \exp \left[-\frac{5}{2} \frac{r^2}{\rho^2} \right]. \end{aligned} \quad (\text{A.3})$$

Thus, we see that $\bar{\psi}\psi$ is sharply peaked, mostly lying within a radius $r \sim \sqrt{2/5} \rho$ or a volume of $(\sqrt{2/5} \rho)^3$, or $\gtrsim 25\%$ of the instanton molecule. This nonlocality will spread the initially forward peaked $\bar{q}q$ wave function over a volume of about 1/4 of the instanton, so we estimate $F = (0.75)^2$ in Sec. 2.4.

Our above estimate holds for the effect of nonlocality in the scalar and pseudoscalar mesons, where its ratio to the size of the instanton is calculated. In the vector and axial-vector the ratio should be to that of the entire molecule, but the nonlocality is also over the whole molecule, and the wave function, due to less binding, will not be so forward peaked as in the π and σ . Thus, we use the same $F = (0.75)^2$.

The possible considerable error in this estimate is important in determining the role of the vectors and axial-vectors in the thermodynamics of the system, but not in our main purpose of constructing continuity in the π and σ masses across T_c .

Ultimately the vector and axial-vector masses may be quantitatively determined for $T \gtrsim T_c$ if the lattice gauge simulation of the Asakawa and Hatsuda type (see Sec. 2.5) are extended to unquenched ones.

References

- [1] G.E. Brown, H.A. Bethe, and P.M. Pizzochero, Phys. Lett. **B263** (1991) 337.
- [2] G.E. Brown, A.D. Jackson, H.A. Bethe, and P.M. Pizzochero, Nucl. Phys. **A560** (1993) 1035.
- [3] T. Hatsuda and T. Kunihiro, hep-ph/0010039; Phys. Lett. **B145** (1984) 7; Phys. Rev. Lett. 55 (1985) 158; Prog. Theor. Phys. **74** (1985) 765.
- [4] T. Schafer and E. V. Shuryak, Phys. Lett. **B356** (1995) 147.
- [5] S. Datta, F. Karsch, P. Petreczky, and I. Wetzorke, Nucl. Phys. Proc. Suppl. **119** (2003) 487.
- [6] M. Asakawa and T. Hatsuda, “ J/ψ and η_c in the deconfined plasma from lattice QCD,” hep-lat/0308034.
- [7] T. Matsui and H. Satz, Phys. Lett. **B178** (1986) 416.
- [8] D. Teaney, J. Lauret, and E. Shuryak, Phys. Rev. Lett. **86** (2001) 4783, see also nucl-th/0110037 (unpublished); P.F. Kolb, P. Huovinen, U.W. Heinz, and H. Heiselberg, Phys. Lett. **B500** (2001) 232.
- [9] D. Teaney, “The effects of viscosity on spectra, elliptic flow and HBT radii”, nucl-th/0301099.
- [10] G. Policastro, D. T. Son and A. O. Starinets, Phys. Rev. Lett. **87** (2001) 081601.
- [11] E. Shuryak and I. Zahed, hep-ph/0307267.
- [12] K. M. O’Hara et al, Science **298** (2002) 2179; T. Bourdel et al, Phys. Rev. Lett. **91** (2003) 020402.
- [13] P. Petreczky, F. Karsch, E. Laermann, S. Stickan, I. Wetzorke, Nucl. Phys. Proc. Suppl. **106** (2002) 513; hep-lat/0110111.
- [14] E. Shuryak and I. Zahed, hep-th/0308073, Phys. Rev. D, in press.
- [15] T. Schäfer and E. V. Shuryak, Rev. Mod. Phys. **70** (1998) 323.
- [16] E. M. Ilgenfritz and E. V. Shuryak, Phys. Lett. B **325** (1994) 263.

- [17] G.E. Brown, L. Grandchamp, C.-H. Lee, M. Rho, hep-ph/0308147.
- [18] C. DeTar, Phys. Rev. **D32** (1985) 276; **D37** (1987) 2378.
- [19] H.A. Weldon, Phys. Rev. **D26** (1982) 2789.
- [20] E V Shuryak, Zh.E.T.F **74** (1978) 408; Sov. Phys. JETP **47** (1978) 212
- [21] M. Harada and K. Yamawaki, Phys. Rep. **381** (2003) 1.
- [22] G.E. Brown, C.-H. Lee and M. Rho, “Chemical equilibration in relativistic heavy ion collisions,” to appear.
- [23] D. Miller, Phys. Reports, in preparation.
- [24] E. V. Shuryak and M. Velkovsky, Phys. Rev. D **50** (1994) 3323.
- [25] T. Schäfer, E. V. Shuryak and J. J. M. Verbaarschot, Phys. Rev. D **51** (1995) 1267; Nucl. Phys., **B412** (1994) 143.
- [26] H.-J. Lee, B.-Y. Park, M. Rho and V. Vento, Nucl. Phys. **A726** (2003) 69; hep-ph/0304066.
- [27] G.E. Brown and M. Rho, Phys. Rev. Lett. **66** (1991) 2720.
- [28] B. Zumino, in *Lectures on Elementary Particles and Quantum Field Theory*, ed. by S. Deser et al (M.I.T. Press 1970) p436.
- [29] K. Langfeld, H. Reinhardt and M. Rho, Nucl. Phys. **A622** (1997) 620.
- [30] V. Koch, E. Shuryak, G.E. Brown, and A.D. Jackson, Phys. Rev. **D46** (1992) 3169
- [31] T.H. Hansson and I. Zahed, Nucl. Phys. **B374** (1992) 277.
- [32] R. Rapp, T. Schäfer, E. V. Shuryak and M. Velkovsky, Phys. Rev. Lett. **81** (1998) 53; M. Alford, K. Rajagopal and F. Wilczek, Phys. Lett. **B422** (1998) 247.
- [33] J. Rafelski, L.P. Fulcher, and A. Klein, Phys. Rept. **38C** (1978) 227.
- [34] G. Breit and G.E. Brown, Phys. Rev. **74** (1948) 1278.
- [35] V. Hund and H. Pilkuhn, J. Phys. **B33** (2000) 1617.
- [36] G.E. Brown, Phil. Mag. **43** (1952) 467.
- [37] E. Fermi, Z.f.Phys. **60** (1930) 320; G. Breit & W. Doermann, Phys. Rev. **36** (1930) 1732.
- [38] E. V. Shuryak and I. Zahed, hep-th/0310031.
- [39] C. Adami, T. Hatsuda, and I. Zahed, Phys. Rev. **D43** (1991) 921.
- [40] V. Koch and G.E. Brown, Nucl. Phys. **A560** (1993) 345.
- [41] D.E. Miller, hep-ph/0008031.

- [42] M. Asakawa, T. Hatsuda, and Y. Nakahara, Nucl. Phys. **A715** (2003) 863c.
- [43] P. Petreczky, hep-ph/0305189.
- [44] G.E. Brown, *"Unified Theory of Nucleon Models and Forces"*, 1967, North Holland Pub. Co., Amsterdam.
- [45] C. Bernard, M.C. Ogilvie, T.A. DeGrand, C. DeTar, S. Gottlieb, A. Krasnitz, R.L. Sugar, and D. Toussaint, Phys. Rev. **D45** (1992) 3854.
- [46] C. Adami and G.E. Brown, Phys. Rep. **234** (1993) 1.